WATER RESOURCES RESEARCH, VOL. 49, 1–8, doi:10.1002/wrcr.20261, 2013

Temperature fluctuations underneath the ice in Diamond Lake, Hennepin County, Minnesota

Gunther Kletetschka,[1,2] Tomas Fischer,[1] Jiří Mls,[1] and Petr Dědeček[3]

Received 19 January 2012; revised 11 March 2013; accepted 15 April 2013.

[1] Diamond Lake in Minnesota is covered every winter with ice and snow providing a modified thermal insulation between water and air. Autonomous temperature sensors, data loggers, were placed in this lake so that hourly measurements could be obtained from the snow-covered ice and water. The sensors that became frozen measured damped and delayed thermal response from the air-temperature fluctuation. Those sensors that were deeper within the snow-covered ice measured continuous, almost constant, temperature values near freezing. Several of them were within the liquid water and responded with a fluctuation of 24 h periods of amplitudes up to 0.2°C. Our analysis of the vertical temperature profiles suggested that the source of periodic water heating comes from the lake bottom. Because of the absence of daily temperature variations of the snow-covered ice, the influence of the air-temperature fluctuation can be ruled out. We attribute the heating process to the periodic inflow of groundwater to the lake and the cooling to the heat diffusion to the overlying ice cover. The periodic groundwater inflow is interpreted due to solid Earth tides, which cause periodic fluctuations of the groundwater pressure head.

Citation: Kletetschka, G., T. Fischer, J. Mls, and P. Dědeček (2013), Temperature fluctuations underneath the ice in Diamond Lake, Hennepin County, Minnesota, *Water Resour. Res.*, *49*, doi:10.1002/wrcr.20261.

1. Introduction

[2] The formation of the ice over lakes and its thickening is a result of air temperature, wind condition, and snow cover [*Adams and Roulet*, 1980; *Adams and Prowse*, 1981; *Bengtsson*, 1986; *Gow and Langston*, 1977; *Jones*, 1969; *Kirillin et al*., 2012]. Because the thermal conductivity of the ice is 1–2 orders of magnitude larger than that of the snow, any thickness of snow over ice provides a significant thermal barrier between temperature of the air and the temperature of the ice. Therefore, the formation of the ice over the lake depends on how much snow covers the lake. Another type of ice is a snow ice formation that is initiated when the mass of snow on the ice causes the ice to sink below the pond's water level, and water flows up through fractures to the ice surface. The thermal resistance of snow becomes a factor when freezing the slush into the snow ice. The phase change regime of ice and its response to air-temperature variability, snow accumulation, and ice formation have been shown to consistently decrease toward the bottom of the ice/water interface [*Gould and Jeffries*, 2005]. Such fluctuation stays within a fraction of the degree, and the ice creates a natural protection from the environmental fluctuation [*Kirillin et al*., 2009, 2012; *Malm et al*., 1997a; *Zdorovennova*, 2009].

[3] The thermal structures in the vicinity of the ice-water and water-sediment interfaces have been given attention in order to characterize the amount of heat released from sediments [*Zdorovennova*, 2009]. When there are no other heat sources (heat exchange with the atmosphere, solar radiation penetrating through the ice, river inflow), the heat flux from the bottom relates to heat accumulation from the previous summer. Because the littoral zone is shallower there is more of the heat captured near the shore than there is in the deeper parts of the lake. Such heat excess from bottom sediments near the shore was reported from small shallow Karelian Lakes [*Malm et al*., 1997a, 1997b]. However, multiple water temperature measurements near bottom sediments in the Lake Vendyurskoe revealed enigmatic temperature structures with 1 day period that could not be explained by baroclinic seiche under the ice [*Zdorovennova*, 2009] with a possibility that such variation may relate to the Poincare type waves [*Kirillin et al*., 2009]. Kirillin also measured details of the temperature variation of ice-covered Lake Müggelsee in Germany and saw the periods of 24, 11, and 8 h in their record. These fluctuations were independent from the amount of snowfall or its melting and indicated that water temperature fluctuations are separated from its solar heating [*Kirillin et al*., 2009].

[4] Observation of the 1 day temperature fluctuation periods in shallow lakes suggests a presence of fundamental forces controlling the winter lake environment. Ice over lakes forms natural protection from environmental extremes important for survival of life forms and may be

[1]Faculty of Science, Charles University in Prague, Prague, Czech Republic.
[2]Institute of Geology, Academy of Science of the Czech Republic, v.v.i., Praha 6 Czech Republic.
[3]Institute of Geophysics, Academy of Science of the Czech Republic, v.v.i., Praha 4 Czech Republic.

Corresponding author: G. Kletetschka, Faculty of Science, Charles University in Prague, Albertov 6, Prague 12843, Czech Republic. (kletetschka@gmail.com)

0043-1397/13/10.1002/wrcr.20261

J_ID: WRCR Customer A_ID: WRCR20261 Cadmus Art: WRCR20261 Ed. Ref. No.: Date: 8-May-13 Stage: Page: 2

critical for development of life, both on Earth and on other bodies of the solar system where the interface between the liquid water and ice is critical for the origin of life. Similar conditions exist not only at the bottoms of numerous lakes whose surface water freezes but also at water/ice interfaces on the top of completely enclosed glacial lakes like the Lake Vostok in Antarctica, similar lakes that are believed to be buried on Mars, as well as the interface of the ice and water on Europa, the moon of Jupiter [*Kletetschka et al*., 2006]. The projected broad relations warrants furthering our understanding of the forces responsible for this not completely understood phenomena. Even though the work by Kirillin and Zdorrovenova was done in fairly shallow lakes, it shows that the fluctuating temperature signal is confined to the sediment/water boundary and disappears toward the ice/water boundary. We chose even shallower lake, the Diamond Lake, Minnesota, with average depth of 2 m.

2. Temperature Monitoring

[5] Autonomous data loggers, iButtons, were utilized to measure not only the speed of the ice growth in the Diamond Lake near Dayton and Rogers, Minnesota (geographical coordinates: longitude −93.506°, latitude 45.201°), but also the environmental conditions that are being kept at the very bottom of the lake ice thickening. The Diamond Lake is small (1.64 km^2) and shallow (maximum depth = 2.44 m, mean depth = 1.98 m). It is 1.4 km long in NS and 1.6 km wide in EW directions, with its 7.24 km shoreline, and stores about 3 km^3 of water (see Figure 1). The bottom of this lake consists of coarse silt sediment. The water is being fed into this lake from the marshes in SW near Rogers town. Water exits in SE via the Diamond Creek flowing into Hyden Lake and further toward the Mississippi River via the Elm Creek. Experimental site was designed near the north shore where the depth of the Diamond Lake was 58 cm. The ice that formed over the lake was periodically covered with snow; whose depth was recorded at KMSP weather station, 40 km southeast from the sensor location (http://mesowest.utah.edu/index.html).

[6] The iButton data loggers (model DS1922L-F50), with a temperature resolution of 0.06°C were used as the autonomous sensors. They contained computer chips enclosed in 16 mm diameter × 6 mm height stainless cylindrical cases. Such package is resistant to environmental hazards such as dirt, moisture, and shock. These devices were made by Embedded Data Systems, LLC (http://www.maxim-ic.com).

[7] Ten sensors were placed in the lake water just after it frozen over on 25 November 2010, when the ice was only 2 cm thick. They were retrieved on 29 March 2011. Sensors were programmed to include the period of interest from 3 December till 19 February. Devices were submerged at 2, 5, 8.5, 12, 17, 22, 24, 26, 28.5, and 30.5 cm below the water level taped to a 1 m of plastic rope, suspended down from the floating container (Figure 1), and anchored with the metal hook at the 58 cm deep bottom. They were programmed to register temperature every 60 min with a resolution of 0.06°C. After data retrieval we checked all

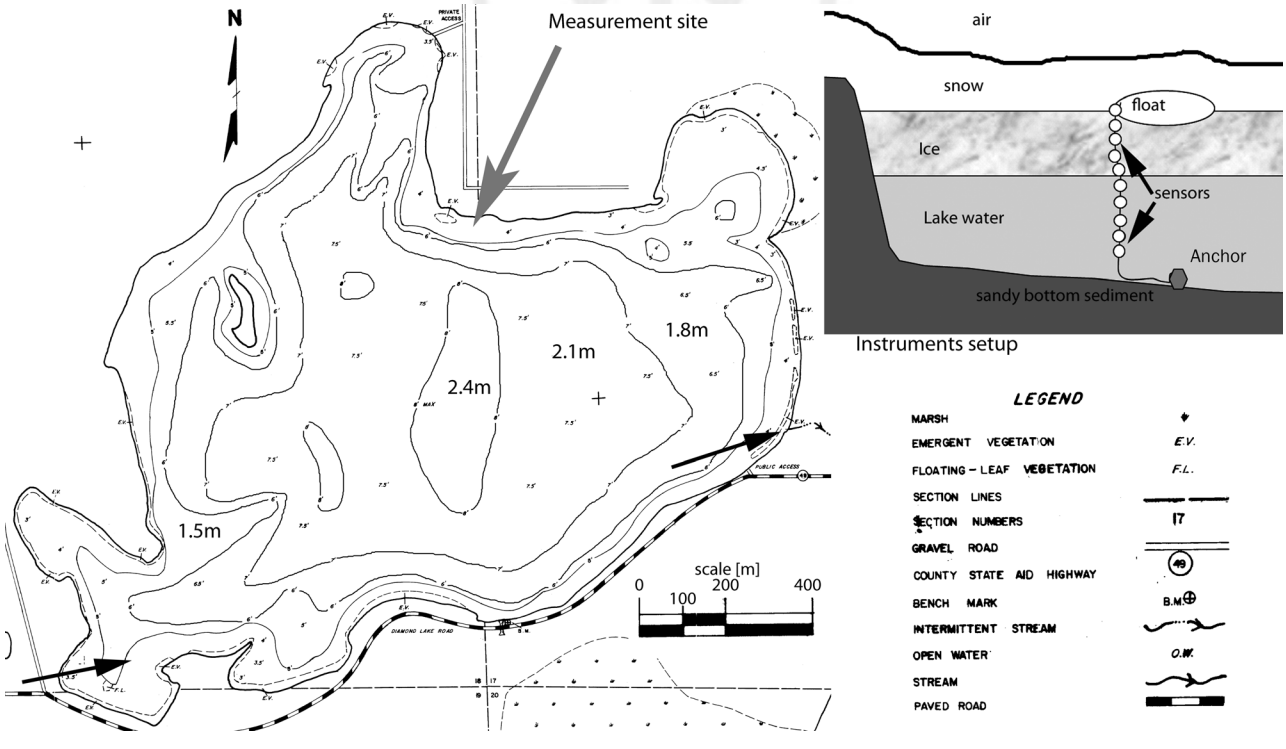

Figure 1. Ten temperature data loggers were placed at the northern shore of the Diamond Lake in Dayton, Minnesota. In the bathymetric map black arrows show the lake water input and output. The gray arrow shows location of the sensors. The upper inset is schematic diagram showing the placement of the sensors. The depth of the lake at the location of the sensors is 58 cm. The shore was 110 cm away. The ice has reached the thickness of 20 cm and stayed constant during most of the measurement period.

ID: muralir Time: 21:28 I Path: N:/3b2/WRCR/Vol00000/130189/APPFile/JW-WRCR130189

J_ID: WRCR Customer A_ID: WRCR20261 Cadmus Art: WRCR20261 Ed. Ref. No.: Date: 8-May-13 Stage: Page: 3

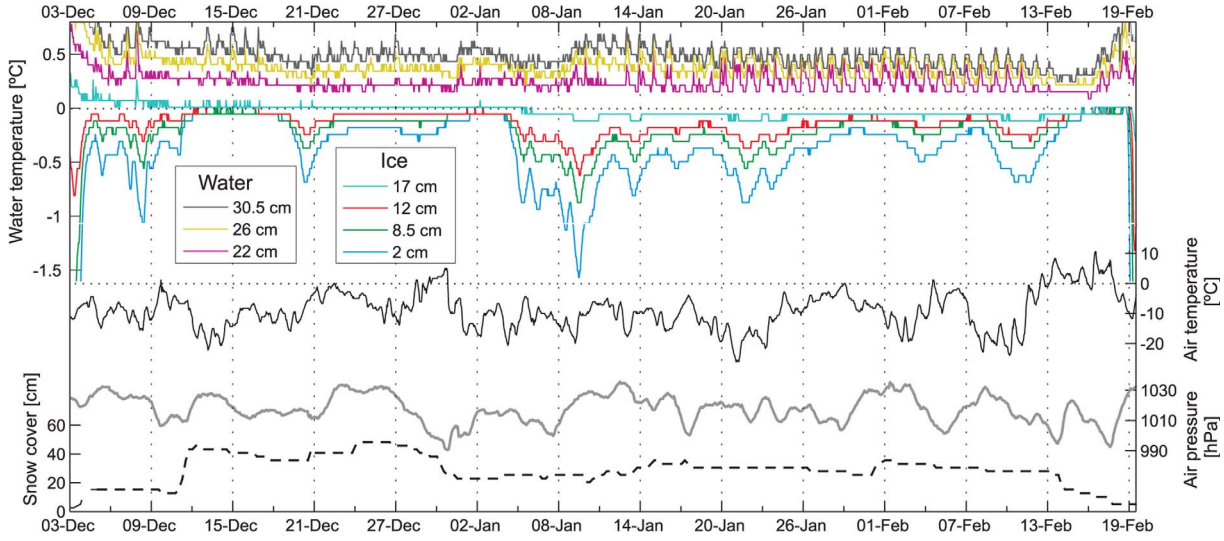

Figure 2. (top) Overall record of temperatures from the eight sensors below the surface, air temperature, barometric pressure, and snow cover (dashed) from Diamond Lake, Minnesota, over the period of 78 days in winter 2010/2011. In the upper section the ice (lower set of four curves) and water (upper set of three curves), temperature was measured by 10 sensors distributed in depths from 2 to 30.5 cm. Curves for data loggers at 5.5 and 28.5 cm are not shown for clarity. The air-temperature curve, snow cover, and barometric pressure records were obtained from the station KMST, 40 km southeast apart.

sensors, and they all worked properly and were suitable for other missions.

3. Data and Results

[8] Temperature records obtained during the period between the two thaws at the beginning of December and the end of February are displayed in Figure 2. This period was characterized by a continuous snow cover and mostly freezing air temperatures. The temperature data separate our devices into two groups (Figure 2): the measurements in ice (sensors at the depths of 2.0, 5.0, 8.5, 12.0, and 17.0 cm; lower group of four curves in the upper region) and measurements in water (sensors at the depths of 22.0, 24.0, 26.0, 28.5, and 30.5 cm; upper group of curves). During the above-mentioned period the temperature in ice at the depth of 2 cm varied between -0.06°C and -1.54°C with minimum after small thaw at the end of December, when the snow cover decreased from 40 down to 20 cm. Temperature at this depth (at the margin of ice) shows strong attenuation of variation of surface air temperature (SAT). This phenomenon is more visible during the month of December due to lower thermal conductivity of powder snow. Several tens of centimeters of powder snow was providing a good thermal insulation for most of the measurement period. The ice temperature at the depth of 17 cm has been monotonous and insensitive to the short- and/or long-term SAT variations. The ice thickness remained between 17 and 22 cm (see constant positive temperature of the sensor at 22 cm and zero-subzero temperatures of the sensor at 17 cm in Figure 2) with the phase boundary moving slightly down during the second half of the observational period (see small decrease of temperature at the depth of 17 cm in Figure 2).

[9] Similar to the temperature in ice, the water temperature (upper group of curves in Figure 2) increased with the depth in general. There are visible short- (days) and long-term (several days) temperature variations in all depths during the course of measurement. Long-term variations are stronger at the deepest level of 30.5 cm near the bottom and are attenuated upward. Short-term variations are attenuated upward too, but only during the first period of the measurement until about 10 January. In the second period the amplitude of variations near the ice increased, whereas the amplitude at the depth of 30.5 cm stayed similar to the first period.

[10] Temperature gradient throughout the observational period was positive (see Figure 3), and the maximum temperature at the depth of 30.5 cm was lower than 1°C. This means that the heat is coming from the lake bottom, and free convection can be ruled out due to the highest water density near the bottom. Such situation suggests conductive heat transfer in the observed temperature profile. We used a 1-D solution of the conductive heat equation in a semi-infinite homogeneous medium [*Carslaw and Jaeger*, 1959]:

$$\frac{\partial T}{\partial t} = k\frac{\partial^2 T}{\partial Z^2} \tag{1}$$

with the periodic boundary condition

$$T(z=0,t) = \mathrm{A}\cos\omega t, \tag{2}$$

where t is the time, z is the depth, T is the temperature, k is the thermal diffusivity, ω is the angular velocity, and A represents the amplitude of the boundary temperature wave. The temperature at depth z and time t can be calculated as

$$T(z,t) = \mathrm{A}e^{-\alpha z}\cos(-\alpha z + \omega t), \tag{3}$$

where $\alpha = \sqrt{\omega/2k}$. It follows that the boundary condition is attenuated exponentially away from the heat source, and

ID: muralir Time: 21:28 I Path: N:/3b2/WRCR/Vol00000/130189/APPFile/JW-WRCR130189

J_ID: WRCR Customer A_ID: WRCR20261 Cadmus Art: WRCR20261 Ed. Ref. No.: Date: 8-May-13 Stage: Page: 4

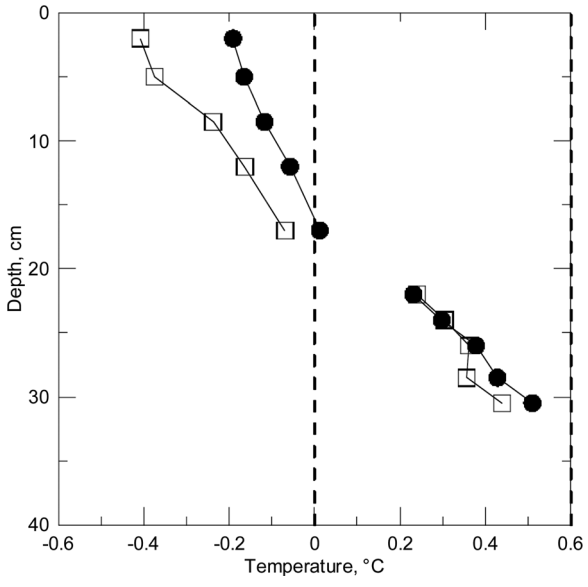

Figure 3. Two sets of average temperature versus lake depth profiles are shown along the thermometer array for 10–30 December 2010 (solid circles) and 15 January to 10 February 2011 (empty squares). Vertical dashed line separates data obtained from lake ice and the data obtained from lake water.

the rate of attenuation depends on the frequency (period). Note that the phase shift increases linearly with the distance from the heat source.

F4 [11] Figure 4 compares the observed and modeled thermal attenuation of amplitude and phase shift during the period from 10 to 30 December (crosses) and period from 15 January to 10 February (triangles). The mean amplitudes and phase shifts were computed over these two periods by solving for the regression constants a_1, a_2, a_3, and a_4 that are part of the trigonometric polynomial $T(t) = a_1 + a_2(\omega t) + a_3 \sin(\omega t) + a_4 \cos(\omega t)$. Solid lines in Figure 4 represent computed amplitude attenuation and phase shift of the observed temperature signal based on equation (3). The source of the periodic temperature change is placed to the depth with the highest amplitude of periodic changes: 30.5 cm in December and 22.5 cm (below the ice) in January/February. The striking fit of the observations and model in December confirms that conductive heat transfer was dominant in the observed temperature profile during that period. However, in January/February the observed and modeled curves of amplitude decay strongly diverge. We suspect that the temperature field during the second observation period is strongly affected by another variable affecting the periodic temperature changes at the water-ice contact. Perhaps, once the lake and tributaries froze over, the water below the ice drained out and left the ice somewhat suspended between the ice and water. This will be a subject of further research.

[12] Similar discrepancy emerged while monitoring the mean temperatures of the investigated depth profile (Figure 3; from 10 to 30 December (squares) and from 15 January to 10 February (circles)). Temperature gradient in water (right side of graph) and ice (left side of graph) was 3.3°C/m and 1.3°C/m over the first period and 2.1°C/m and 2.4°C/m

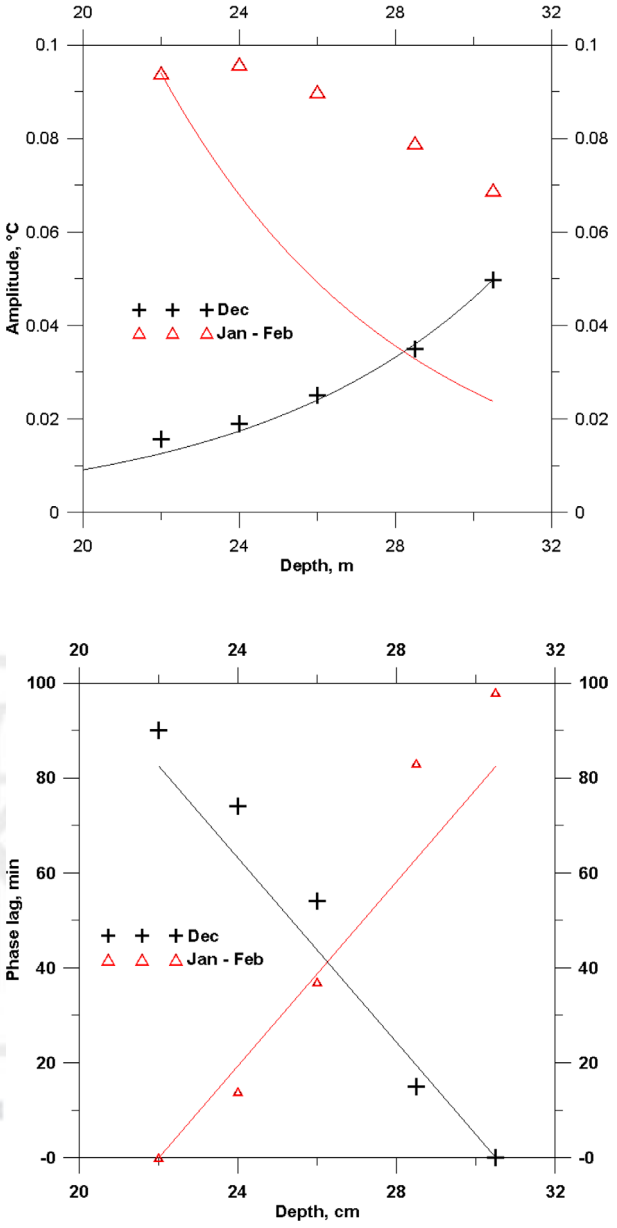

Figure 4. Observed and modeled attenuation of (top) amplitude and (bottom) phase shift of the daily temperature oscillations during the period from 10 to 30 December (crosses) and period from 15 January to 10 February (triangles). Solid lines represent computed amplitude attenuation and phase shift of observed temperature signal based on equation (3).

over the second period, respectively. The corresponding heat flux is lower in water than in ice with 2.0 and 2.9 W/m^2 during the first period, but 1.3 and 5.3 W/m^2 during the second one, respectively. Calculation assumed only a conductive heat transfer. The values of the temperature gradient (heat flux) in water are in good agreement with other lakes in Minnesota and Wisconsin [*Fang and Stefan*, 1996]. The discrepancy between the heat flux in water and ice during January and February can be connected with the phase changes in the water-ice transition zone. The heat transfer during this period

ID: muralir Time: 21:28 I Path: N:/3b2/WRCR/Vol00000/130189/APPFile/JW-WRCR130189

J_ID: WRCR Customer A_ID: WRCR20261 Cadmus Art: WRCR20261 Ed. Ref. No.: Date: 8-May-13 Stage: Page: 5

cannot be explained by simple conduction theory and is beyond the scope of this paper.

[13] We summarize the outcomes of Figures 2–4 as follows:

[13] (1) The influence of daily air-temperature fluctuations on the water temperature variations can be ruled out for two reasons. First, the air-temperature variations show prevailing long periods caused by ambient weather changes, and the corresponding daily period is minor. Second, the air-temperature variation is separated from the first sensor in ice by a 20 to 40 cm thick layer of snow. At the ice depth of 2 cm, the amplitudes of air-temperature variation completely disappear. Only the long-term air-temperature variations are visible in the uppermost sensors, because the longer periods are less attenuated.

[13] (2) There is a positive temperature gradient during the whole snow-covered period (Figure 3). It suggests that the source of the heat and cold (heat sink) should be below and above of the device array, respectively. The daily temperature maxima occur at about midnight, and this disqualifies the possible origin of the water temperature variations as a response to the Sun radiation.

[13] (3) Periodic temperature variations in the water at the depth of 30.5 cm are visible during the whole observation period between the thaws. The variations are attenuated upward during the month of December, and the conductive heat transfer plays substantial role. During the month of January and the first half of February the variations in the upper part of the sensor chain under the ice cover became stronger due to other mechanisms of unknown origin.

[14] During the snow-covered period, air-temperature variations do not affect the dynamics of water temperature field. During the thaw when the snow disappears, the solar heating becomes more effective, and the radiation-driven convection starts to develop. As a result, the temperature gradient in the close vicinity of the ice-water interface is nearly permanent for most of the winter, and the heat flux from water to ice varies slightly in time [see *Malm et al*., 1997a, 1997b]. This is in agreement with our measurements and clearly visible in Figure 3 where the mean temperature gradient between two detectors just under the ice cover is similar during both of the above-mentioned periods (December and January/February). Warming from the bottom is driven by the heat stored in the bottom sediments during the summer [*Fang and Stefan*, 1996]. This process starts immediately when the average temperature of the air drops below the lake bottom temperature [*Zdorovennova*, 2009].

[15] We examine the periodicity of the temperature records by spectral analysis (Figure 5a). The amplitude spectrum of the temperatures shows few pronounced maxima at 24.0, 12.1, and 8.0 h. While the 24 h period is undisputable, we consider the relevance of the 8 and 12 h periods questionable. The reason is the spiky character of the temperature records caused by the insufficient amplitude resolution of the digitized temperature, which generates higher harmonics.

4. Discussion

[16] Two possible physical mechanisms are considered that could be responsible for periodical discharge of the warmer water to the lower part of the measured profile. The first are the basin-scale internal waves that may affect the temperature distribution in shallow lakes. Among them, two kinds of waves can be distinguished. The first are the baroclinic seiches. The period of a baroclinic seiche is given [*Gill*, 1982; *Zdorovennova*, 2009] as

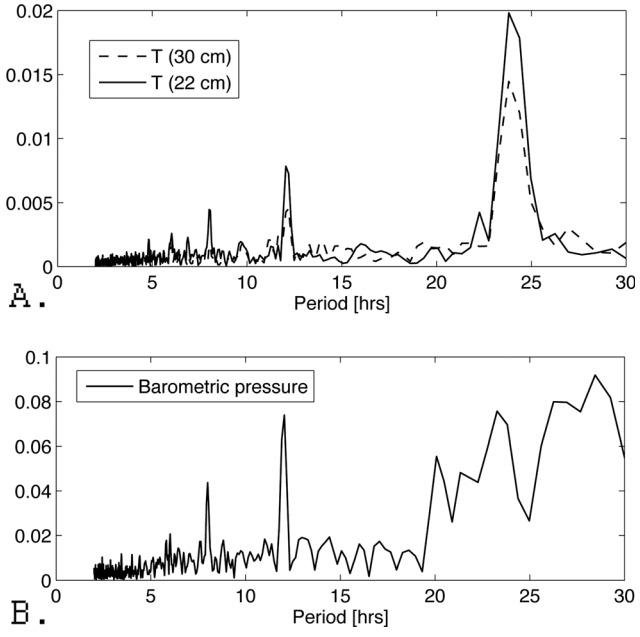

Figure 5. Amplitude spectra show (a) temperature and (b) barometric records at depths of 22 and 30 cm for the period 20 January to 10 February 2011 when the amplitude of oscillations was the highest.

$$T_1 = \frac{2\pi L}{H\sqrt{\frac{g}{\rho}\frac{d\rho}{dz}}}, \tag{4}$$

where the index 1 denotes mode of the baroclinic seiche, L is the maximum length of the lake basin, H is the mean depth of the lake minus the ice thickness, g is the gravity acceleration, ρ is the average water density, and its derivative is average vertical density gradient.

[17] Another kind of basin-scale internal waves is connected with inertial frequency and the Earth rotation, which generate waves of the geostrophic inertia-gravity character of two frequencies [*Kirillin et al*., 2009] split around the inertia-gravity waves into supercritical (Poincare wave) and subcritical (Kelvin wave) modes propagating in opposite directions [*Gill*, 1982]. Kelvin wave affects the water-sediment interface in the littoral zone, where it can produce shear turbulence and resuspension, while the Poincare wave produces water movements in the middle of the lake [*Kirillin et al*., 2009]. Dissipation of these rotational waves has longer time scales than simple seiches and for elliptical basin can last up to 1 week [*Antenucci and Imberger*, 2001a, 2001b].

[18] The second mechanism is the tidal accelerations that act on both the solid Earth and water bodies, generating time-dependent changes of the water level. The combination of the Moon and Sun motions with the Earth rotation

ID: muralir Time: 21:29 I Path: N:/3b2/WRCR/Vol00000/130189/APPFile/JW-WRCR130189

J_ID: WRCR Customer A_ID: WRCR20261 Cadmus Art: WRCR20261 Ed. Ref. No.: Date: 8-May-13 Stage: Page: 6

results in a complex time dependence of tidal acceleration, which can be expressed as a sum of harmonic tidal constituents with prevailing diurnal and semidiurnal periods. Unlike the oceans, the groundwater is not attracted directly by the tidal forces. Instead, the solid Earth tides generate deformation of the rock environment, which results in cyclic opening and closing of the pore space [*Fischer et al*., 2006; *Rojstaczer and Riley*, 1990]. It results in oscillations of pressure head causing Darcian flow of groundwater that periodically changes its direction.

[19] For the selection of the more likely mechanism we first verify the possible effect of seiches by examining their period, which depends on the lake geometry and density gradients. Using approach of *Zdorovennova* [2009], the period of a baroclinic seiche can be evaluated using equation (4). In Figure 6 we show the dependence of seiche period on the bottom temperature and mean lake depth for the maximum length of the lake basin $L = 1.5$ km and average water density $\rho = 999.957$ kg/m^3. Average water density gradient was estimated from the bottom and ice interface temperatures, and the lake depth H was considered in the range 0.5–2.5 m. It appears that if for the bottom temperature ranges from 0°C to 4°C the seiche period varies from about 2 days and more. However, the bottom temperature probably does not exceed 1° C based on the measured temperature profile and the mean lake bottom temperatures measured in Minnesota [*Fang and Stefan*, 1998]. Therefore, the seiche period would exceed 3 days, which is in contrast with the exact period of the temperature oscillations of 24 h found in the spectrum in Figure 5a. This disqualifies the seiches as the possible driving force and supports tides as the most likely driving mechanism of observed temperature variations.

[20] Next we analyze the possible influence of tides. The mechanism that could convert the tidal acceleration to the oscillations of pressure head may be complex as it strongly depends on the structure of the underlying layers, particularly in the presence of fractures and/or faults. Such mechanisms were presented in mathematical models [*Bodvarss*, 1970; *Ondovcin et al*., 2012]. In our approach we assume a presence of semipervious aquitard beneath the lake bottom. Lake sediment layer does not allow for any measurable amount of flow through the whole surface of the bottom. However, the communication between the underlying aquifer and the lake water is possible through preferential zones. As the water enters the lake bottom via these zones, it spreads laterally over the lake's floor due its higher density, while the heat in vertical direction moves conductively.

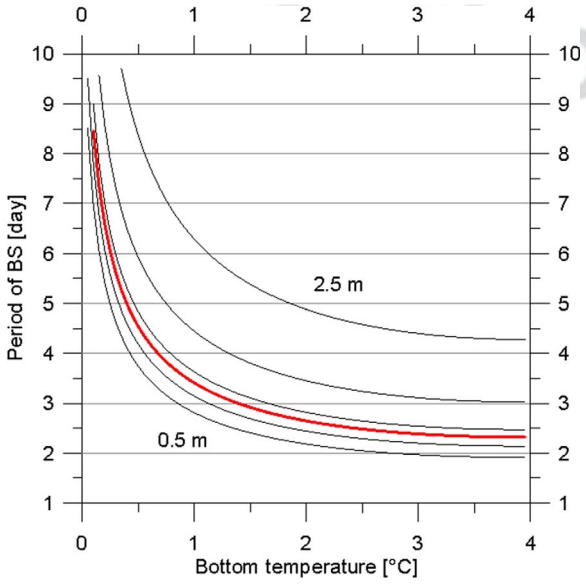

Figure 6. Period of baroclinic seiches as a function of bottom temperature and lake depth (equation (4)) calculated for $L = 1.5$ km and temperature-dependent water density. The bold line refers to the mean depth of the lake of 1.7 m.

[21] For tidal analysis of periodic inflow of groundwater we compared the theoretical Earth tides with the temperature records. We have evaluated the tidal effects for the region of interest in Minnesota at latitude 45.201°N and longitude −93.504°E. The ocean load was not taken into account because of its negligible effect at a distance larger than 1000 km from the sea. The tidal potentials and the vector tidal acceleration for the investigated time period were calculated using a program [*Skalsky*, 1990] based on Tamura's [*Tamura*, 1987] development. Additionally, the volumetric strains and the longitudinal strains in the N, E, and Z directions were evaluated using a slightly modified ETERNA program [*Wenzel*, 1993] based on the global elastic tide model. The selected tidal characteristics are shown along with the temperature records in Figure 7 and indicate a possible relationship between the temperature data and the modeled solid Earth tides. To quantify this relation a cross correlation of the time series in the time lag interval from −4 to +4 days was determined (Figure 8). In terms of the tidal force, the maximum cross correlation of 0.49 at the phase lag of 50 h and the maximum anticorrelation of −0.44 at the lag of −10 h were found for the vertical component of the tidal force. The solid Earth strains show the maximum correlation of 0.45 for the phase lag of about 9 h and maximum anticorrelation of −0.44 for the phase lag of 21 h. Here the positive phase lag corresponds to a delay of the temperature maxima after the maxima of the Earth tides.

[22] The cross-correlation factor of about 0.4 is not insignificant, namely, in view of the spiky temperature record, which ranges within the first digits of the sensors' temperature resolution of 0.06°C. Note that the cross correlation with tides shows global maxima within the interval of 0–2 days (Figure 8). Especially, the tidal force shows sharp global maximum. This suggests that both the daily period and the low-frequency modulation period present in Earth tides are transferred to the temperature oscillations. The similar values of positive correlation and anticorrelation for both the vertical component of the tidal force and for the volumetric tidal strains do not allow for clear identification of the driving mechanisms of the temperature variations. The fact that the temperature maxima follow the maxima of the Earth tides with a delay of several hours supports the hypothesis that the groundwater is injected from the underlying aquifer due to the tidal effects.

[23] In addition to the Earth tides acting as a driving force for periodic temperature variations, the effect of atmospheric tides also should be examined. In contrast to

ID: muralir Time: 21:29 I Path: N:/3b2/WRCR/Vol00000/130189/APPFile/JW-WRCR130189

J_ID: WRCR Customer A_ID: WRCR20261 Cadmus Art: WRCR20261 Ed. Ref. No.: Date: 8-May-13 Stage: Page: 7

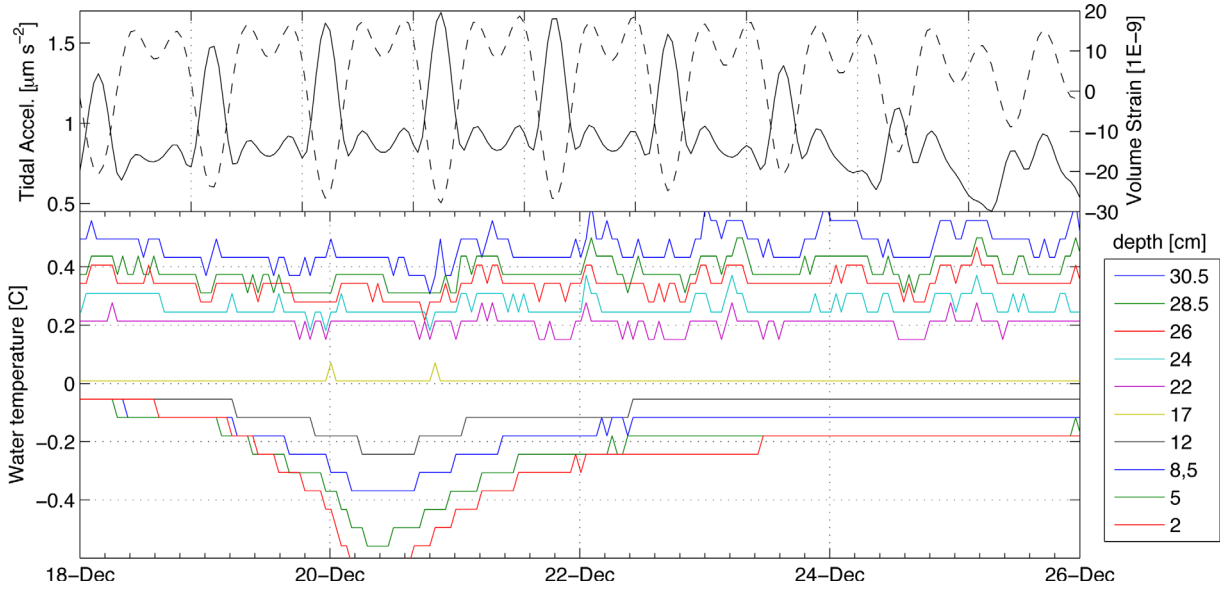

Figure 7. Detailed segment of all of the temperature data from 10 data loggers and Earth tides for the period 18–26 December 2010. Solid line is the vertical component of tidal acceleration, and dashed line is the volume strain. The numbers in the legend are the depths of the sensors underneath the water level in centimeters.

Earth tides, the atmospheric tides are driven by periodic solar heating of the atmosphere with a strongly prevailing 12 h period [*Chapman and Lindzen*, 1970; *Covey et al*., 2011] as the influence of the equator region dominates. Despite the fact that the tidal variations at middle latitudes are masked by air pressure variations due to weather changes [*Lindzen and Chapman*, 1969], the 12 h period is present in the spectrum of Figure 5 for the barometric pressure record in Minnesota (compare the long-period variations dominating the barometric record in Figure 2 with its spectrum in Figure 5). We infer that the influence of atmospheric tides is negligible because their dominant period of 12 h vanishes in the temperature records where 24 h period dominates.

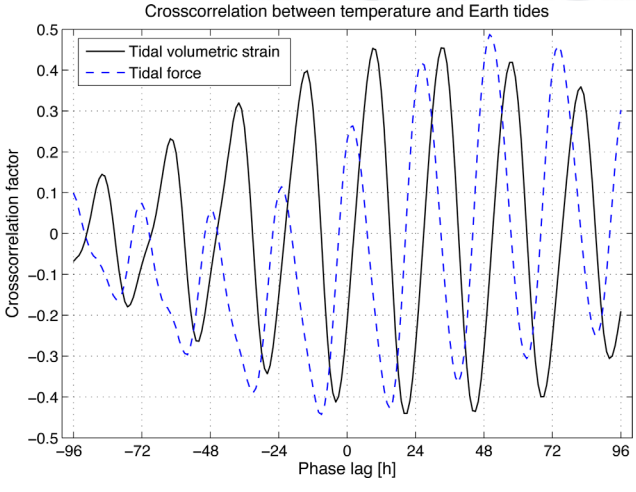

Figure 8. Cross-correlation function between volumetric strain and temperature. Positive phase corresponds to delay of temperature at 30.5 cm depth after Earth tides (tidal force, dashed line; volumetric strain, full line) for the observational period shown in Figure 7.

[24] The water table fluctuation due to Earth tides is a complex function of the hydraulic parameters of the aquifers. Larger fluctuations are expected if the formation has a higher permeability and a lower specific yield [*Rojstaczer and Riley*, 1990]. This could be the case of the investigated area, whose surficial geology includes silt containing till with specific yield typically below 10% [*Johnson*, 1967]. It should be noted that many observations show that the tidal behavior of wells is strongly laterally dependent [*Mrlina et al*., 2003]. Such dependence could be caused by a lateral heterogeneity of the aquifer whose parts are connected with a deeper fault system that is exposed to a cyclic stress perturbation due to the Earth tides.

5. Conclusions

[25] Analysis of the vertical profile of the lake water temperatures for a period of 3 months during the winter shows that water temperature under the ice oscillates by 0.2°C with a daily period, while the temperature of the ice shows only the long-period changes reflecting the variation of the air temperature. The temperature variation from shallow to deeper parts of the lake is governed by the periodic thermal conduction during the first month. However, during the second and the third month we identified the existence of the periodic variable insulation condition responsible for variable heat conduction at the ice-water interface and sharp deviation from regular periodic heat conduction observed during the first month.

[26] We have provided two models explaining the periodic thermal oscillation near the lake ice-water interface. The first model is considering the baroclinic seiches. Specific lake geometry indicates the period of the first mode of

ID: muralir Time: 21:29 I Path: N:/3b2/WRCR/Vol00000/130189/APPFile/JW-WRCR130189

J_ID: WRCR Customer A_ID: WRCR20261 Cadmus Art: WRCR20261 Ed. Ref. No.: Date: 8-May-13 Stage: Page: 8

barometric seiches is larger than 3 days, which is far from what we observed. The second model, the influence of Earth tides, appears more consistent with the data because the temperature period matches the 1 day period the Earth tides.

[27] We propose that the Earth tides may periodically change the porosity of the underlying aquifer, squeezing periodically the warmer water out toward the surface. This process would be responsible for the water temperature variations by the periodic inflow of the warmer groundwater. Because the water stays below the 4°C at the lake bottom, the heat is transferred by conduction, which we confirmed by comparing the measured data with the theoretical model. The tidal influence on lake temperature oscillation is supported by both spectral analysis of tides and cross correlation of measured temperature series with the modeled tidal force and volumetric strains.

[28] Observations of the tide and/or baroclinic seiche-induced temperature changes have yet not been reported and open an important angle when estimating the thermal budget under the lake ice. These changes speed up the transfer of heat from the bottom to the ice cover and serve as an important variable for existence of life in completely covered water bodies with ice (Lake Vostok) or similar once on other planets (Mars) and moons (Europa).

[29] **Acknowledgments.** The authors thank Emi Ito and two anonymous reviewers for their comments improving this manuscript. The authors also thank to Jim and Joyce Young for their cooperation when using their private shore of the Diamond Lake and helping with the inserting and retrieving the temperature sensors. Finally, GK wants to thank Peter Wasilewski and Allen Lunsford for suggesting the idea of lake temperature measurements, Kristyna Cizkova for help with the graphics, and Susanne Maeder for help with obtaining bathymetry maps. The tidal strains were calculated by Lumír Skalský. This work was supported by the Research Plan of the Institute of Geology AS CR, v.v.i. CEZ AV0Z30130516, Research Projects of Czech Ministry of Education LK 21303 and MSM 0021620855, Grant Agency of the Czech Academy of Sciences under grant IAA300120905, and Grant Agency of the Czech Republic under grant 205/09/1879.

References

Adams, W. P., and T. D. Prowse (1981), Evolution and magnitude of spacial patterns in the winter cover of temperate lakes, *Fennia*, *169*(2), 343–359.

Adams, W. P., and N. T. Roulet (1980), Illustration of the roles of snow in the evolution of the winter cover of a lake, *Arctic*, *33*(1), 100–116.

Antenucci, J. P., and J. Imberger (2001a), Energetics of long internal gravity waves in large lakes, *Limnol. Oceanogr.*, *46*(7), 1760–1773.

Antenucci, J. P., and J. Imberger (2001b), On internal waves near the high-frequency limit in an enclosed basin, *J. Geophys. Res.—Oceans*, *106*(C10), 22,465–22,474.

Bengtsson, L. (1986), Spatial variability of lake ice covers, *Geogr. Ann.*, *68A*(1–2), 113–121.

Bodvarss, G. (1970), Confined fluids as strain meters, *J. Geophys. Res.*, *75*(14), 2711–2718.

Carslaw, H. S., and J. C. Jaeger (1959), *Conduction of Heat in Solids*, 505 pp., Oxford Univ. Press, New York.

Chapman, S., and R. S. Lindzen (1970), Atmospheric Tides, 200 pp. AQ7

Covey, C., A. G. Dai, D. Marsh, and R. S. Lindzen (2011), The surface-pressure signature of atmospheric tides in modern climate models, *J. Atmos. Sci.*, *68*(3), 495–514.

Fang, X., and H. G. Stefan (1996), Long-term lake water temperature and ice cover simulations/measurements, *Cold Reg. Sci. Technol.*, *24*(3), 289–304.

Fischer, T., P. Kalenda, and L. Skalsky (2006), Weak tidal correlation of NW-Bohemia/Vogtland earthquake swarms, *Tectonophysics*, *424*(3–4), 259–269.

Gill, A. E. (1982), *Atmospheric-Ocean Dynamics*, Academic, New York.

Gould, M., and M. Jeffries (2005), Temperature variations in lake ice in central Alaska, USA, in *Annals of Glaciology*, vol. *40*, edited by D. R. MacAyeal, pp. 89–94. AQ8

Gow, A. J., and D. Langston (1977), Growth history of lake ice in relation to its stratigraphic, crystalline and mechanical structure, Rep., 1–24 pp. AQ9

Johnson, A. I. (1967), *Specific yield-compilation of specific yields for various materials*, U.S. Geol. Surv. Water Supply Pap. 1962-D, pp. 1–74.

Jones, J. A. A. (1969), The growth and significance of white ice at Knob Lake, *Quebec, Can. Geogr.*, *13*(4), 354–372.

Kirillin, G., C. Engelhardt, S. Golosov, and T. Hintze (2009), Basin-scale internal waves in the bottom boundary layer of ice-covered Lake Muggelsee, Germany, *Aquat. Ecol.*, *43*(3), 641–651.

Kirillin, G., et al. (2012), Physics of seasonally ice-covered lakes: A review, *Aquat. Sci.*, *74*(4), 659–682.

Kletetschka, G., S. A. Getty, M. Shields, J. Li, V. Mikula, and P. Wasilewski (2006), Microbial origin of life on Europa, *Orig. Life Evol. Biosph.*, *36*(3), 328–330.

Lindzen, R. S., and S. Chapman (1969), Atmospheric tides, *Space Sci. Rev.*, *10*(1), 3–188.

Malm, J., A. Terzhevik, L. Bengtsson, P. Boyarinov, A. Glinsky, N. Palshin, and M. Petrov (1997a), Temperature and salt content regimes in three shallow ice-covered lakes: 1. Temperature, salt content, and density structure, *Nord. Hydrol.*, *28*(2), 99–128.

Malm, J., A. Terzhevik, L. Bengtsson, P. Boyarinov, A. Glinsky, N. Palshin, and M. Petrov (1997b), Temperature and salt content regimes in three shallow ice-covered lakes: 2. Heat and mass fluxes, *Nord. Hydrol.*, *28*(2), 129–152.

Mrlina, J., A. Spicak, and L. Skalsky (2003), Non-seismological indications of recent tectonic activity in the West Bohemia earthquake swarm region, *J. Geodyn.*, *35*(1–2), 221–234.

Ondovcin, T., J. Mls, and L. Herrmann (2012), Mathematical modelling of tidal effects in groundwater, *Transp. Porous Media*, doi:10.1007/s11242-11012-10056-11243. AQ10

Rojstaczer, S., and F. S. Riley (1990), Response of the water level in a well to earth tides and atmospheric loading under unconfined conditions, *Water Resour. Res.*, *26*(8), 1803–1817.

Skalsky, L. (1990), Calculation of theoretical values of the tidal strain components with respect to their practical use, paper presented at Seminar Advances in Gravimetry, Geophys. Inst., Slovak Acad. of Sci., Bratislava, Smolenice, December 10–14.

Tamura, Y. (1987), A harmonic development of the tide-generating potential, *Bull. Inf. Marees Terr.*, *99*, 6813–6855.

Wenzel, H. G. (1993), ETERNA, in *Program Manual*, Geodaetisches Inst., Karlsruhe, Germany.

Zdorovennova, G. E. (2009), Spatial and temporal variations of the water-sediment thermal structure in shallow ice-covered Lake Vendyurskoe (Northwestern Russia), *Aquat. Ecol.*, *43*(3), 629–639.

ID: muralir Time: 21:29 I Path: N:/3b2/WRCR/Vol00000/130189/APPFile/JW-WRCR130189

Author Queries

AQ1 Please check whether the affiliations and the correspondence are correct as set.

AQ2 Please define KMSP at first use.

AQ3 Please include the year along with date and month throughout this paper.

AQ4 Please provide complete bibliographic details for the reference Fang and Stefan [1998] in the list.

AQ5 Please check whether the edit made to the sentence "We have evaluated the tidal effects (" retains the intended meaning.

AQ6 Please define ETERNA, if an abbreviation.

AQ7 Please provide publisher name and location for the reference Chapman and Lindzen [1970].

AQ8 Please provide publisher name and location for the reference Gould and Jeffries [2005].

AQ9 Please provide report number for the reference Gow and Langston [1977].

AQ10 Please provide volume and page numbers for the reference Ondovcin et al. [2012].

AQ11 Please note the figures have been renumbered to maintain sequential order.

AQ12 COMP: Please set the artworks of Figures 6, 7, and 8 as Figures 7, 8, and 6, respectively.

USING e-ANNOTATION TOOLS FOR ELECTRONIC PROOF CORRECTION

Required software to e-Annotate PDFs: Adobe Acrobat Professional or Adobe Reader (version 8.0 or above). (Note that this document uses screenshots from Adobe Reader X)
The latest version of Acrobat Reader can be downloaded for free at: http://get.adobe.com/reader/

Once you have Acrobat Reader open on your computer, click on the Comment tab at the right of the toolbar:

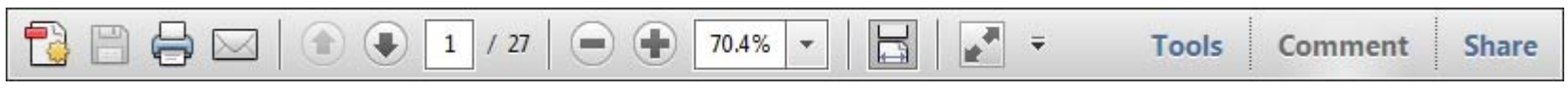

This will open up a panel down the right side of the document. The majority of tools you will use for annotating your proof will be in the Annotations section, pictured opposite. We've picked out some of these tools below:

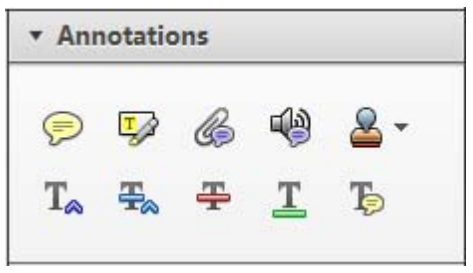

1. Replace (Ins) Tool – for replacing text.

Strikes a line through text and opens up a text box where replacement text can be entered.

How to use it

- Highlight a word or sentence.
- Click on the Replace (Ins) icon in the Annotations section.
- Type the replacement text into the blue box that appears.

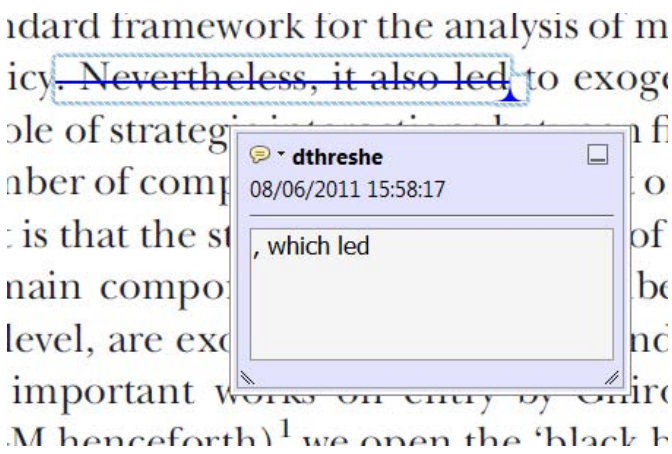

2. Strikethrough (Del) Tool – for deleting text.

Strikes a red line through text that is to be deleted.

How to use it

- Highlight a word or sentence.
- Click on the Strikethrough (Del) icon in the Annotations section.

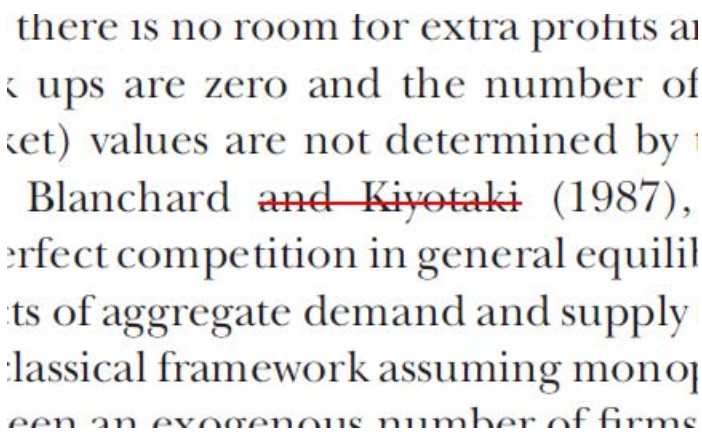

3. Add note to text Tool – for highlighting a section to be changed to bold or italic.

Highlights text in yellow and opens up a text box where comments can be entered.

How to use it

- Highlight the relevant section of text.
- Click on the Add note to text icon in the Annotations section.
- Type instruction on what should be changed regarding the text into the yellow box that appears.

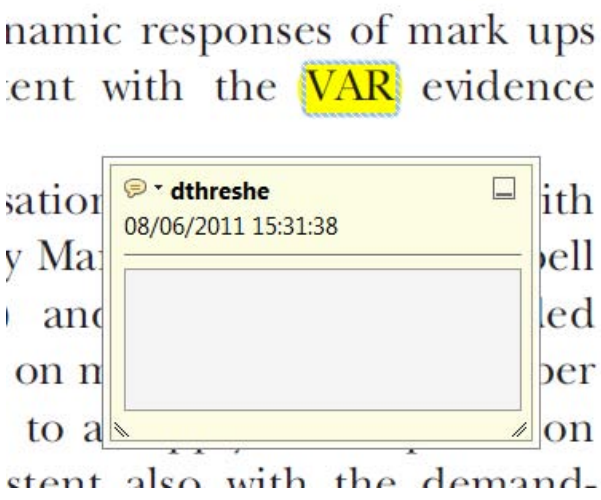

4. Add sticky note Tool – for making notes at specific points in the text.

Marks a point in the proof where a comment needs to be highlighted.

How to use it

- Click on the Add sticky note icon in the Annotations section.
- Click at the point in the proof where the comment should be inserted.
- Type the comment into the yellow box that appears.

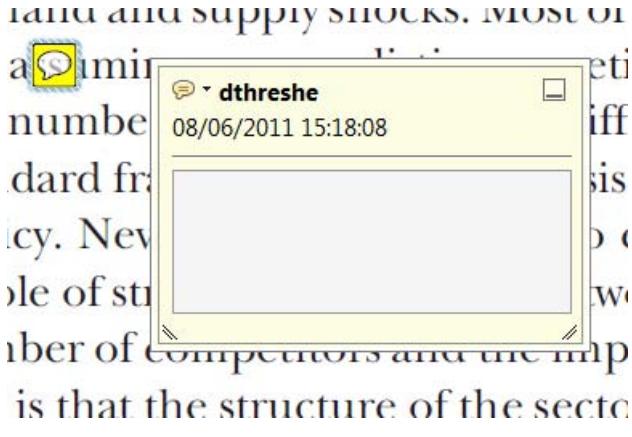

WILEY-BLACKWELL

USING e-ANNOTATION TOOLS FOR ELECTRONIC PROOF CORRECTION

5. Attach File Tool – for inserting large amounts of text or replacement figures.

Inserts an icon linking to the attached file in the appropriate pace in the text.

How to use it

- Click on the Attach File icon in the Annotations section.
- Click on the proof to where you'd like the attached file to be linked.
- Select the file to be attached from your computer or network.
- Select the colour and type of icon that will appear in the proof. Click OK.

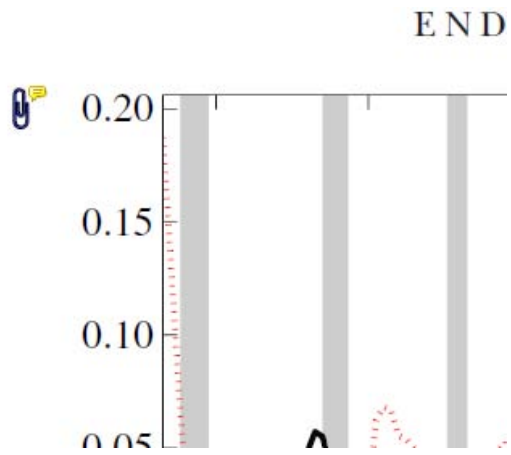

6. Add stamp Tool – for approving a proof if no corrections are required.

Inserts a selected stamp onto an appropriate place in the proof.

How to use it

- Click on the Add stamp icon in the Annotations section.
- Select the stamp you want to use. (The Approved stamp is usually available directly in the menu that appears).
- Click on the proof where you'd like the stamp to appear. (Where a proof is to be approved as it is, this would normally be on the first page).

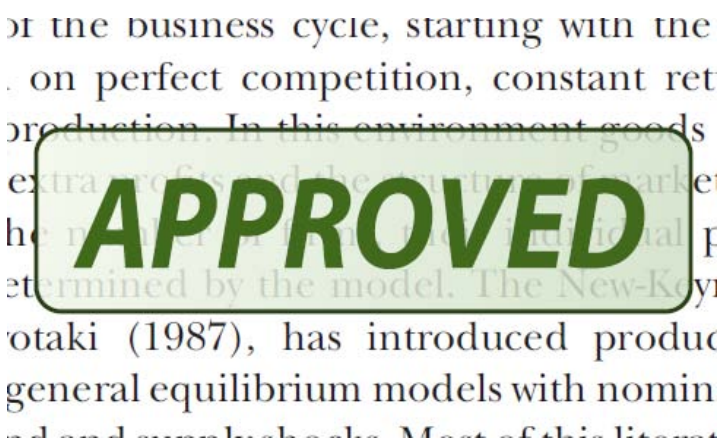

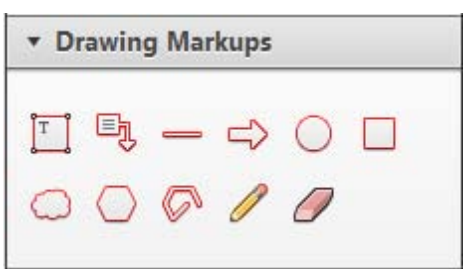

7. Drawing Markups Tools – for drawing shapes, lines and freeform annotations on proofs and commenting on these marks.

Allows shapes, lines and freeform annotations to be drawn on proofs and for comment to be made on these marks..

How to use it

- Click on one of the shapes in the Drawing Markups section.
- Click on the proof at the relevant point and draw the selected shape with the cursor.
- To add a comment to the drawn shape, move the cursor over the shape until an arrowhead appears.
- Double click on the shape and type any text in the red box that appears.

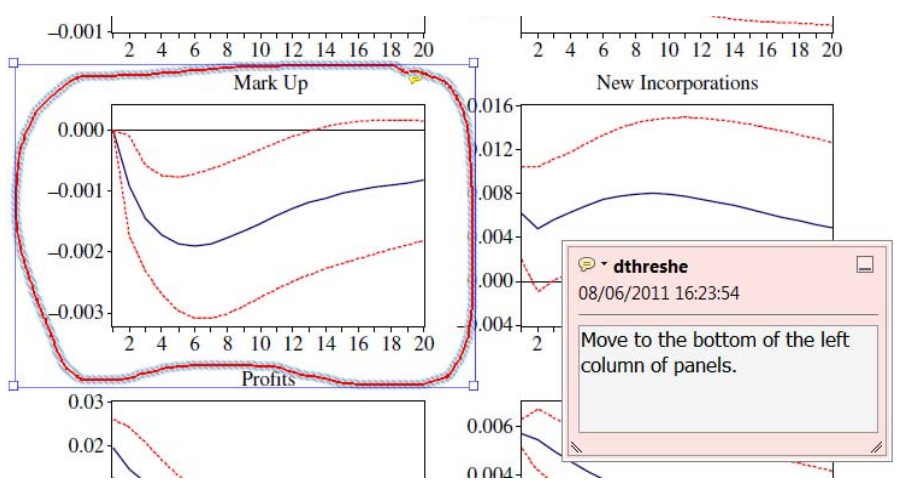

For further information on how to annotate proofs, click on the Help menu to reveal a list of further options: